Harnessing an adapted strain of Clostridium carboxidivorans to unlock hexanol production from carbon dioxide and hydrogen in elevated-pressure stirred tank reactors

Terms of use:

Publisher copyright

(Article begins on next page)

19 February 2025

Harnessing an adapted strain of *Clostridium carboxidivorans* to unlock hexanol production from carbon dioxide and hydrogen in elevated-pressure stirred tank reactors

G. Antonicelli [a,b], N. Vasile [a,b], E. Piro [a,e], S. Fraterrigo Garofalo [c], B. Menin [a,d], F. Verga [b], F. Pirri [a,c], V. Agostino [a,*]

[a] *Centre for Sustainable Future Technologies, Fondazione Istituto Italiano di Tecnologia, Via Livorno 60, Turin 10144, Italy*
[b] *Department of Environment, Land and Infrastructure Engineering, Politecnico di Torino, Corso Duca degli Abruzzi 24, Turin 10129, Italy*
[c] *Department of Applied Science and Technology, Politecnico di Torino, Corso Duca degli Abruzzi 24, Turin 10129, Italy*
[d] *Institute of Agricultural Biology and Biotechnology, National Research Council, CNR-IBBA, Via Alfonso Corti 12, Milano 20133, Italy*
[e] *Department of Life Sciences and Systems Biology, University of Turin, Via Verdi 8, Turin 10124, Italy*

HIGHLIGHTS

- Process development with *Clostridium carboxidivorans* in elevated-pressure reactor.
- Definition of crucial gas feeding strategies influencing the product metabolism.
- Unprecedented hexanol carbon selectivity (60%)
- Highest hexanol titer (3.7 gL^{-1}) and productivity (0.9 $gg_{CDW}^{-1}d^{-1}$) from H_2 and CO_2.
- Enhanced caproate production (1.6 gL^{-1}) from *Clostridium carboxidivorans*.

GRAPHICAL ABSTRACT
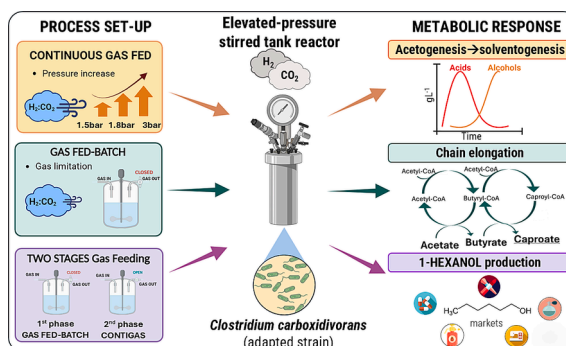
ARTICLE INFO

ABSTRACT

To successfully scale-up the production of bio-based building blocks through CO_2 and H_2-based gas fermentation, it is crucial to deeply understand and control the microbial catalyst response to the bioreactor environment. This study investigates the effects of key process parameters, such as CO_2 and H_2 partial pressures, gas feeding strategies, and mixture composition, on the production pathways of an evolved *Clostridium carboxidivorans* strain. The ultimate goal is to optimize 1-hexanol production in elevated-pressure stirred-tank reactors. Continuous gas feeding enhanced acetogenic and solventogenic metabolisms, while gas-limited conditions promoted chain elongation to caproic acid. An optimized process, combining an initial gas-limited step followed by a continuous gas phase, increased 1-hexanol production, achieving a maximum biomass-specific productivity of 0.9 g g_{CDW}^{-1} day^{-1}. In-situ product extraction improved 1-hexanol carbon selectivity to an unprecedented 60 %. These

findings demonstrate the potential of CO_2 and H_2-fed fermentation to produce high-value chemicals other than ethanol and acetate.

1. Introduction

Carbon-intensive materials and chemicals are mainly derived from fossil sources, with no viable alternative currently available for their replacement. As a consequence, the increasing demand for carbon-negative manufacturing processes has triggered research into the development of novel sustainable technologies (IPCC 2023). Among them, gas fermentation represents a distinctive biotechnological solution able to generate bio-based products from readily available gaseous waste streams. Lanzatech (https://lanzatech.com/; Köpke and Simpson 2020), Synata Bio (https://synatabio.com/) and Jupeng Bio (http://www.jupengbio.com/) are the three company providers of gas fermentation technology for ethanol production using refinery, ferroalloy and steel industry off-gases or syngas derived from waste gasification. There are currently six commercial ethanol production plants in operation using Lanzatech technology. Gas fermentation technology is based on the utilization of acetogenic bacteria which can grow on C1-gases and H_2 due to their metabolism: the Wood Ljungdahl pathway (WLP). Acetogens naturally generate valuable products such as short chain organic acids, alcohols and diols (Bae et al., 2022; Kim et al., 2023; Sun et al., 2019). Their product metabolism occurs in two stages: the acetogenesis pathway primarily supports growth and acetate production with minimal alcohol generation, while the solventogenesis pathway converts accumulated acetate or, less frequently, gases into ethanol (Wirth and Dürre 2021). Although acetate and ethanol are their primary products, some acetogenic *Clostridium* strains can produce medium-chain acids, such as butyrate and caproate *via* chain elongation pathway (Wirth and Dürre 2021; Wu et al., 2024) and their corresponding alcohols, i.e., butanol and hexanol, respectively (Fernández-Blanco et al., 2023; Thunuguntla et al., 2024a; Thunuguntla et al., 2024b).

Hexanol holds significant interest due to its versatility and widespread applications across various market sectors, including food, pharmaceuticals, cosmetics, flavor&fragrance, detergents, coatings, and as a finishing agent in the leather industry (Fernández-Naveira et al., 2017b). Its production relies on energy-intensive chemical processes generating significant CO_2 emissions (i.e., hydroformylation followed by hydrogenation, Ziegler alcohol synthesis and Fischer-Tropsch synthesis) and using fossil-based or palm oil-based substrates (Xu et al., 2024). There are currently no commercially available sustainable alternative technologies for hexanol production. Only a few research studies have been reported on glucose-based bio-hexanol production using engineered *Escherichia coli* strains, resulting in very low productivity. This is likely due to the complex and lengthy biosynthetic pathway of hexanol, which place a significant metabolic burden on strains that do not naturally possess this biosynthetic route (Huang and Ma, 2023).

The acetogen *Clostridium carboxidivorans* P7 wild type (WT) proved to be an interesting strain for its ability to naturally produce hexanol from C1-gases (Doll et al., 2018; Fernández-Naveira et al., 2017a–c; Liou et al., 2005; Phillips et al., 2015). The highest hexanol titer reported so far by this strain (5 g L^{-1}) has been achieved in serum bottles with CO as substrate and *in-situ* solvent extraction (Oh et al., 2023). Nevertheless, in this study, 65 % of the dissolved CO was converted into CO_2, and only 25 % into hexanol. The process has also been investigated in lab-scale bioreactors by various research groups, employing always syngas or CO-based gas mixtures as feedstocks. In these studies, different operational parameters, such us pH (Abubackar et al., 2018; Doll et al., 2018; Lanzillo et al., 2024), gas impurities, (Rückel et al., 2021, 2022) and mixotrophic cultivation with glucose (Vees et al., 2022) have been evaluated. Additionally, various configurations of bioreactors have been explored, including hollow fibers (Shen et al., 2014b) or monolithic biofilm reactors (Shen et al., 2014a), horizontal rotating packed bed

biofilm reactors (Shen et al., 2017) and gas lift reactor (Riegler et al., 2019). However, when transitioning from serum bottles to reactors, the hexanol production performances declined, with a maximum hexanol titer of less than 1 g L^{-1} (Fernández-Naveira et al., 2017a), shifting to ethanol production.

There are very few studies in the literature regarding hexanol bioproduction from CO_2 and H_2 mixtures (without CO). This is because acetogenic *Clostridium* strains grow much less effectively on CO_2 and H_2 mixtures compared to CO (Antonicelli et al., 2023). Our previous study demonstrated the efficacy of the Adaptive Laboratory Evolution (ALE) methodology in enhancing the strain proficiency to utilize CO_2 as the carbon source and H_2 as the electron donor. Similarly, Thunuguntla and colleagues recently reported the growth of *C. carboxidivorans* WT with CO_2 and H_2 in serum bottles (Thunuguntla et al., 2024a; Thunuguntla et al., 2024b). Nevertheless, no studies have yet explored bioreactor systems fed with CO_2 and H_2 using *C. carboxidivorans* strains. Developing lab-scale bioreactor processes is essential for assessing the feasibility of scaling-up innovative value chains. Lab-scale gas fermentation processes development for CO_2 and H_2 valorization into liquid products, have only been reported using the acetogenic *Clostridium* strains *C. autoethanogenum* and *C. ljungdahlii,* mainly producing acetate and ethanol (Heffernan et al., 2020; Hermann et al., 2020; Mock et al., 2015; Oswald et al. 2018).

To address this gap, the present work investigated the physiology of the promising *C.carboxidivorans* hex21 strain (Antonicelli et al., 2023) in H_2 and CO_2-fed bioreactors. Since the use of H_2 can limit the microorganism's availability of reducing equivalents due to its lower water solubility at atmospheric pressure (0.79 mM at 25 °C and 1 atm) compared to CO_2 (34.08 mM at 25 °C and 1 atm) (Fernández-Naveira et al., 2017b), elevated-pressure stirred tank reactors have been employed. In particular, the authors aim to explore how CO_2 and H_2 partial pressures, along with gas feeding modes, could impact the three product pathways of the strain, with a special focus on hexanol production. The strain's varying availability of CO_2 and H_2 has proven to be crucial for controlling acetogenesis, solventogenesis and chain elongation. A two-stage gas-feeding process was developed, where the conditions in the first fermentation phase were optimized for caproate production, and the conditions in the second step were optimized for subsequent hexanol production. Eventually, the effectiveness of *in-situ* solvent extraction (oleyl alcohol) to mitigate hexanol toxicity on cells was evaluated for the first time in elevated-pressure bioreactor system. The highest hexanol carbon selectivity (60 %) *via* gas fermentation ever reported was achieved, with a promising cell-specific productivity of 0.9 g_{HexOH} g_{CDW}^{-1} day^{-1}.

2. Material and methods

2.1. Microorganism, medium and fermentation conditions

The adapted strain *C. carboxidivorans* hex21, previously developed in our laboratory (Antonicelli et al., 2023), was used in this work. Medium composition, culture conditions in serum bottles and cryopreservation are described in Antonicelli et al., 2023. For the bioreactor inoculum preparation, the strain was re-activated from glycerol stock in heterotrophic culture condition (5 g L^{-1} glucose) in 250 mL serum bottles (OEA labs, UK) with 25 mL of nominal volume, at 37 °C in static condition. The late exponential phase biomass was transferred two times in autotrophic cultivation conditions (H_2:CO_2 ratio of 4:1, 1.75 bar pressure, 25 °C temperature, 100 rpm horizontally shaken). The second autotrophic pre-culture, in the exponential growth phase, was used as the inoculum, with a volume adjusted to achieve an optical density of

0.2 in the bioreactor. Gas fed-batch experiments in 250 mL serum bottles with 25 mL of medium with caproic acid were carried out by re-pressurizing the bottles daily at 1.75 bar. Different concentrations of 98 % pure caproic acid (Alfa Aesar, (0.5 gL^{-1}, 1 gL^{-1} and 2 gL^{-1}) were added after the inoculum using a 25 μL micro syringe (Hamilton, USA). The pH was adjusted to 6 with an anaerobic stock of 4 M NaOH.

2.2. Gas fermentation in stirrer tank reactors

The bioreactor experiments were carried out in three 0.5 L high-pressure stirred tank reactors (STR) (H.E.L Group, United Kingdom) (see Supplementary material). Key parameters such as pressure, temperature and pH were monitored using probes (Hamilton, USA). Pressure control was achieved through a proportional back pressure regulation valve. The gas was supplied in the fermentation broth using a micro sparger located at the vessel base, with flow rates regulated by mass flow controllers (Bronkhorst, Netherland). Cultures were performed with 200 rpm of agitation using a 0.25 L of working volume. A temperature of 25 °C was employed to enhance the solventogenic phase as demonstrated in previous works (Antonicelli et al., 2023; Ramió-Pujol et al., 2015). In experiments with pH control, a 2 M NaOH solution and a piston pump (Eldex, USA) were used. Before the inoculum, the bio-reactors were sparged overnight with N_2 and subsequently with CO_2 and H_2 for 24 h. Tests with continuous gas flow were performed with a gas mixture of either 80 % H_2 and 20 % CO_2 (ratio 4:1) or 67 % H_2 and 33 % CO_2 (ratio 2:1) sparged at 15 mL min^{-1}. The H_2 to CO_2 ratios of 4:1 and 2:1 were selected as most suitable for hexanol and caproate production, respectively (Antonicelli et al., 2023). For the assessment of the effect of gas partial pressures on the production profile of the evolved strain (section 3.1), three different total pressures were evaluated with continuous gas flow, keeping a 4:1 H_2:CO_2 gas ratio: 1.5 bar for both condition 1 (p_{H2} = 0.6 bar; p_{CO2} = 0.15 bar; p_{N2} = 0.75 bar) and condition 2 (p_{H2} = 1.2 bar; p_{CO2} = 0.3 bar); 1.8 bar for condition 3 (p_{H2} = 1.44 bar; p_{CO2} = 0.36 bar); and 3 bar for condition 4 (p_{H2} = 2.4 bar; p_{CO2} = 0.6 bar). Tests with the gas fed-batch configuration were performed at 1.8 bar with either a 4:1 or 2:1 H_2:CO_2 gas ratios. The gas fed-batch configuration consisted of a repeated filling of gas in the headspace of reactors. When the pressure dropped from 1.8 bar to 1.2 bar due to the gas consumption, the system automatically started supplying gas with a rate of 15 mL min^{-1}. Once the pressure returned to 1.8, the system automatically halted the gas flow. The two stages gas feeding strategy consisted in a first gas fed-batch phase followed by a continuous gas feeding phase (conti-gas). The first stage aimed to enhance caproate production in a gas limiting step condition; the second stage aimed to convert caproate into hexanol by providing both H_2 and CO_2 with a faster dissolution rate. The off-gas was monitored by microGC analyses (described in Section 2.3). Experiments were carried out in liquid batch conditions. Samples for optical dentisy (OD$_{600}$) and high-performance liquid chromatography (HPLC) measurements were taken every day. For *in-situ* hexanol-selective extraction (see Section 3.3), 6 % v/v of oleyl alcohol (OAL) (80–85 % purity) was added to the medium as the solvent.

2.3. Analytical methods

The organic acids and alcohols concentrations in the samples were measured *via* HPLC. The methods have already been described in detail in our previous work (Antonicelli et al., 2023). The bioreactor off-line gas analysis was conducted with a two channels Micro gas chromatograph Agilent 490 (Agilent, USA), also described in Antonicelli et al., 2023. The composition of alcohols present in the oleyl alcohol phase was determined using an Agilent 8890 GC system equipped with a flame ionization detector (GC-FID). The alcohols concentration quantified in oleyl alcohol layer was normalized for the total nominal volume in the reactor as shown in Oh et al. (2023). A H_2 flow rate of 30 mL min^{-1} and an airflow rate of 350 mL min^{-1} were used. The flow rate of the carrier gas (He) was set at 2.5 mL min^{-1}. The temperature of the injection port

and detector were set at 250 and 300 °C, respectively. The oven temperature was initially programmed at 40 °C for 5 min, then the temperature was raised to 200 °C at a rate of 5 °C min^{-1} and finally increased to 250 °C. The injection volume was 1 μL in the split 25:1 injection mode. A capillary column Agilent CP7681 (25 m × 320 μm × 5 μm) was employed. Standards and samples were diluted with acetone.

2.4. Calculation of main fermentation metrics

Cell dry weight (CDW), volumetric and specific productivities were calculated as described in Antonicelli et al. (2023). The carbon selectivity was calculated as the ratio between moles of a specific product on a carbon basis (C-mols) and the total C-mols recovered across all quantified products at the end of fermentation, including biomass, which was also treated as a product. A biomass molecular weight of 24.6 g mol^{-1} (chemical formula: $CH_{1.8}O_{0.5}N_{0.2}$) was used for calculation (Villadsen et al., 2011). Both the volumetric (q_{CO2}) and cell-specific (r_{CO2}) carbon uptake rates were calculated by considering the total C-mmol fixed into products and biomass measured by HPLC analysis every day of fermentation.

2.5. Computational model description

The computational model developed in MATLAB simulates the mass transfer dynamics of H_2 and CO_2 in a stirred tank reactor under abiotic conditions. The model addresses the mass balance in both the gas and liquid phases, accounting for the interphase mass transfer between gas and liquid, driven by the concentration gradients (Tarraran et al., 2022). The solubility of the gases is modeled at 25 °C using Henry's law, which allows for the calculation of gas concentrations in the liquid phase at different partial pressures (Sander, 2023). Empirical equations were implemented to calculate the volumetric mass transfer coefficient (k_La), incorporating factors such as gas superficial velocity, power input, and reactor geometry (Garcia-Ochoa and Gomez, 2009; Akita and Yoshidal 1973; Van't Riet, 1979; Zedníková et al. 2018). For each gas (H_2 and CO_2), two distinct k_La values were modeled to account for the operational differences between conti-gas and gas fed-batch configurations. As described in detail in the Supplementary Material, the equations for k_La incorporate key parameters of the system, including the geometry of the reactor, which is a CSTR equipped with two Rushton turbines for effective mixing and a microporous sparger for fine gas dispersion (the reactor dimensions are reported in the Supplementary Materials). The equations also account for the working pressure, which influences the solubility of the gases and the driving force for mass transfer, as well as the liquid properties, such as viscosity and density, which affect the hydrodynamic behavior of the system. Additional operational parameters include the gas inlet velocity, which determines the gas flow characteristics within the reactor, the rotation speed of the impeller, which governs the turbulence and mixing intensity, and the specific physical properties of the gases, such as diffusivity and solubility. Together, these factors ensure a comprehensive representation of the mass transfer dynamics under the two different operational mode in abiotic conditions. The results from these simulations include the dissolution times for both gases, the dissolution rates, and the total quantities of H_2 and CO_2 solubilized across all operational scenarios. The model was applied to two different case studies to explore various operational scenarios. In the first study, the dissolution times of H_2 and CO_2 were evaluated under continuous gas flow conditions at different partial pressures while maintaining a constant H_2 to CO_2 ratio of 4:1. The second study compared the dissolution times in continuous gas flow and fed-batch configurations, starting at 1.2 bar and reaching 1.8 bar, with varying H_2 to CO_2 ratios (4:1 and 2:1). In all cases, a total gas flow rate of 15 mL min^{-1} was used, with the mixing provided by an impeller operating at 200 rpm. The results from these simulations include the dissolution times for both gases, the dissolution rates, and the total quantities of H_2 and CO_2 solubilized across all operational scenarios.

2.6. Statistical analysis

All the data presented for the serum bottle experiments are shown as mean values of triplicate experiments ± standard error of the mean (SEM). All the data presented for the bioreactor experiments derive from duplicate experiments shown as mean values ± standard error of the mean (SEM), except for the data from the 2:1 H_2:CO_2 ratio in conti-gas condition (Section 3.2) and from the 2:1 gas fed-batch experiment (Section 3.2 Fig. 3), which are as a single experiment. The GraphPad Prism 9.3.1 (USA) software was used for data analysis and plot elaboration. The statistical analysis was carried out as described in Antonicelli et al. (2023).

3. Results and discussion

3.1. Evaluation of the effect of H_2 and CO_2 partial pressures on the strain production profile

The effect of p_{H2} and p_{CO2} on *C. carboxidivorans* growth and production profile has never been studied. Consequently, those are the first operational parameters we investigated. The bioreactor experiments with *C. carboxidivorans*_hex21 were carried out with a continuous gas flow, by maintaining a H_2:CO_2 ratio of 4 to 1 and by varying the gas partial pressures. Four conditions were tested in a 7-day fermentation test: p_{H2} = 0.6 bar, p_{CO2} = 0.15 bar and p_{N2} = 0.75 bar, total pressure 1.5 bar (condition 1); p_{H2} = 1.2 bar and p_{CO2} = 0.30 bar, total pressure 1.5 bar (condition 2); p_{H2} = 1.44 bar and p_{CO2} = 0.36 bar, total pressure 1.8 bar (condition 3) and p_{H2} = 2.4 bar and p_{CO2} = 0.6 bar, total pressure 3 bar (condition 4).

Despite having similar growth profiles (Fig. 1A), higher biomass
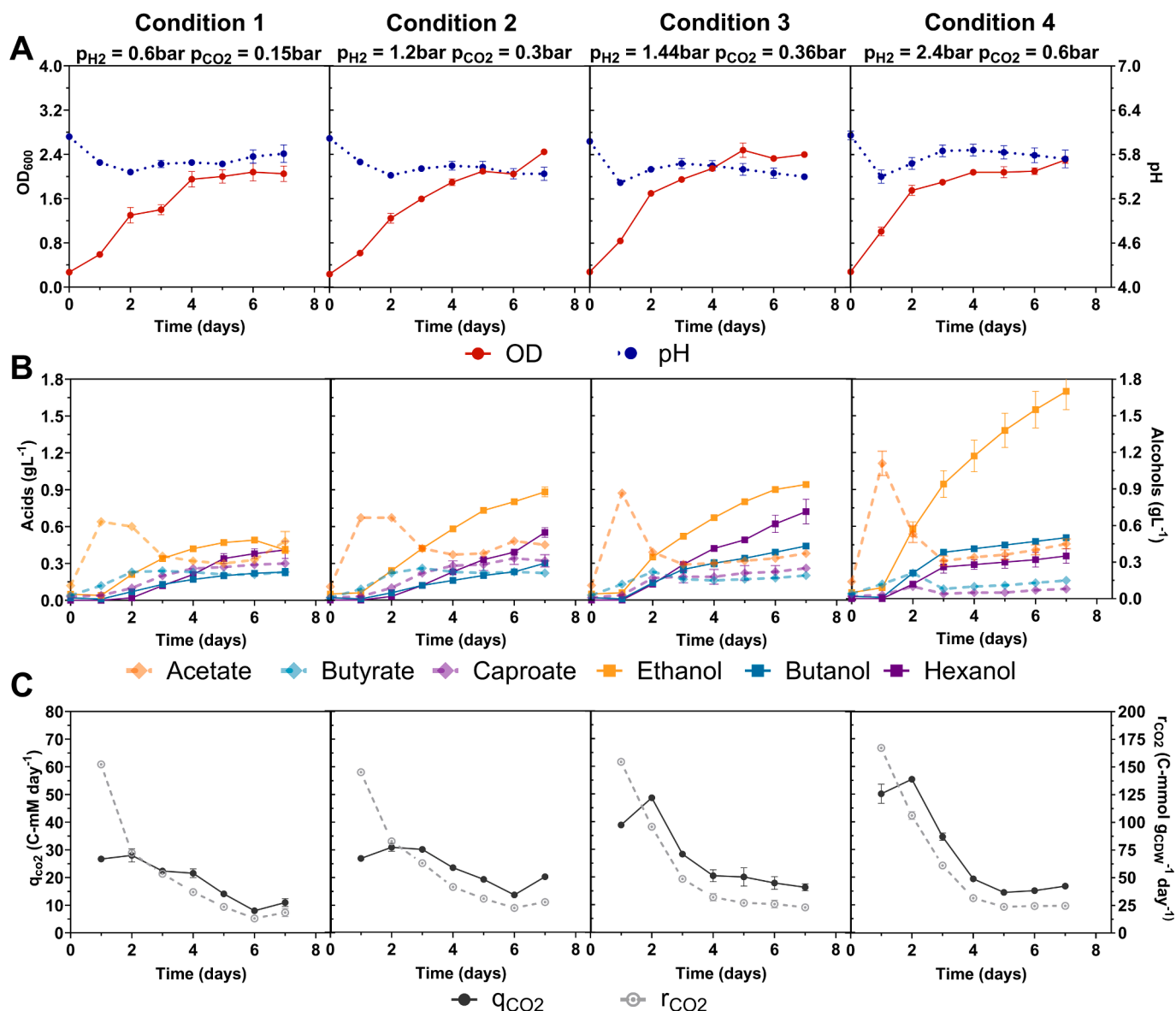
Fig. 1. Growth, product profiles and C-uptake rate of *C. carboxidivorans*_hex21 with different H_2-CO_2 partial pressures. (A) Optical density profiles (solid red lines), pH profiles (dotted blue lines) and (B) products profiles. Acetate, butyrate and caproate are respectively shown as light orange, light blue and light purple diamond shapes with dotted lines. Ethanol, butanol and hexanol are respectively shown as orange, blue and purple squares with solid lines. (C) Specific CO_2 uptake rate (r_{CO2}) (C-mmol g_{CDW}^{-1} day^{-1}) is shown as light gray dotted lines; volumetric CO_2 uptake rate (q_{CO2}) (C-mM day^{-1}) is shown as dark solid line. All data represent the average ± standard error of the mean (SEM) of duplicate experiments.

concentrations were reached on the second day of fermentation in higher partial pressure conditions (conditions 3 and 4) (Table 1). This result is consistent with the volumetric carbon uptake rate (q_{CO2}) of day 2 (Fig. 1C). Specifically, the q_{CO2} of conditions 3 (48.7 ± 0.7 C-mM day^{-1}) and 4 (55.6 ± 0.7 C-mM day^{-1}) were respectively 1.6- and 1.8-fold higher than the q_{CO2} of condition 2 (30.7 ± 1.2 C-mM day^{-1}) (q_{CO2} P value: condition 3 = 0.0002 (***); condition 4 < 0.0001 (****)). It should be highlighted that the cell-specific CO_2 uptake rate (r_{CO2}) was also influenced by the increased gas partial pressures. The highest r_{CO2} was observed in condition 4 on the first day of fermentation (1.7 ± 2 C-mmol g_{CDW}^{-1} day^{-1}) (Table 1, Fig. 1C). This finding implies that the increased availability of CO_2 and H_2 in the liquid medium (see Supplementary Material) improved the biomass growth until the second day of fermentation and positively influenced the CO_2 uptake rate.

The observed results are quite different from the behavior of *C. ljungdahlii* and *A. woodii* at high p_{H2} and p_{CO2}, reported in recent literature. The p_{H2} increase seems to restrict microbial growth while the increment of the CO_2 partial pressure (p_{CO2}) seems to shift microbial metabolism towards formic acid production (Oswald et al. 2018; Tarraran et al., 2023). In contrast to what was observed with *C. ljungdahlii* and *A. woodii*, increasing gas partial pressures significantly enhanced both acetate and ethanol production of *C. carboxidivorans*_hex21 (Fig. 1B), and only trace amounts of formic acid were observed (data not shown). A possible explanation can be related to the different portfolio of *C. carboxidivorans*_hex21 hydrogenase enzymes compared to C. *ljungdahlii* and *A. woodii* (Di Leonardo et al., 2022; Schuchmann et al., 2018). Hydrogenases are crucially involved in the WLP enzymatic reaction of CO_2 reduction to formate. Future ohmics and biochemical studies are necessary to elucidate the reasons for this different behavior among acetogens. Concernig *C. carboxidivorans*_hex21, when the partial pressures were doubled from condition 2 to condition 4, acetate accumulation on the first day of fermentation was significantly enhanced,

with an acetate spike of 1.1 ± 0.10 gL^{-1}, which is 1.6 times higher than the 0.67 ± 0.03 gL^{-1} of acetate observed in condition 2 (P value = 0.0371 (*)). This is consistent with the highest biomass concentration achieved in condition 4, as acetate production in acetogens is closely correlated with cell growth. Increased gas partial pressures also led to higher acetate consumption rates after the first day of fermentation, resulting in enhanced ethanol production (Fig. 1B) (Table 1). In condition 4, a max r_{EtOH} of 0.04 ± 0.01 g_{EtOH} g_{CDW}^{-1}h^{-1} and a final ethanol titer of 1.70 ± 0.15 gL^{-1} were achieved. The higher acetate concentration and the enhanced availability of reducing equivalents, due to the improved H_2 solubility at higher pressures, could explain the improved ethanol production performances of condition 4 (see Supplementary Material).

Increased p_{H2} and p_{CO2} did not stimulate the chain elongation pathway of the strain and the subsequent production of longer-chain alcohols (butanol and hexanol). In particular, the hexanol carbon selectivity was halved from 26 % of condition 3 to 13 % of condition 4 (P value = 0.0225 (*)). On the other hand, the ethanol carbon selectivity increased from 24 % (condition 3) to 44 % (condition 4) (P value = 0.0289 (*)). However, a linear increase of hexanol titer and maximum r_{HexOH} from condition 1 to condition 3 was observed (Table 1), reaching a maximum titer of 0.72 ± 0.10 gL^{-1} in condition 3. This outcome suggests that the production of hexanol requires precise regulation of H_2 and CO_2 partial pressures and gas concentration in the liquid phase.

3.2. Control of product metabolic pathways through the gas-feeding dosing

Based on the results described above, it is clear that different dissolved amounts of CO_2 and H_2 in the liquid medium affect the cell growth and the three product pathways (acetogenesis, solventogenesis and chain elongation) (Fernández-Naveira et al., 2017a–c; Vees et al., 2022) of the adapted strain. Therefore, two additional parameters that can influence the dissolution and the availability of CO_2 and H_2 for the biocatalyst were investigated: the gas feeding strategy (fed-batch vs conti-gas) and different H_2 to CO_2 ratio (2:1 vs 4:1), utilizing a total gas pressure of 1.8 bar (Fig. 2).

As observed in the serum bottle experiments of Antonicelli et al. (2023), an H_2 to CO_2 ratio of 4:1 resulted in higher production of alcohols relative to acids, compared to the 2:1 ratio condition (Fig. 2B). Specifically, the ratio of acids to alcohols for the four conditions tested were as follows: 2:1 gas fed-batch equal to 18.91; 4:1 gas fed-batch equal to 1.73; 2:1 conti-gas equal to 0.31; 4:1 conti-gas equal to 0.70. The computational modelling of CO_2 and H_2 dissolution rate in abiotic condition (see Section 2.5 of Materials and Methods and Supplementary Material) demonstrates a faster abiotic CO_2 dissolution rate in conti-gas compared to gas fed-batch mode (see Supplementary Material). In both the 4:1 and 2:1 continuous gas fermentation, ethanol was the major compound produced (0.67 gL^{-1} and 0.60 gL^{-1}, respectively), followed by hexanol. Furthermore, acid consumption was observed, with acetate being the most produced and subsequently reduced acid (Fig. 2B). The abiotic CO_2 dissolution rate of conti-gas exceeded the CO_2 uptake rate of *C. carboxidivorans*, and no CO_2 percentage variations were observed in the reactor off-gas analysis compared to the gas-in. As a matter of fact, with both 2:1 and 4:1 conti-gas conditions, the abiotic CO_2 dissolution rate was respectively 14-fold and 5-fold higher compared to the maximum q_{CO2} measured on the second day of fermentation (see Supplementary Material, Fig. 2C). It is therefore clear that, when CO_2 and H_2 are continuously available in the liquid phase (conti-gas), acetogenesis is the first pathway stimulated, followed by solventogenesis, mainly leading to ethanol production. Under this condition, the chain elongation of acetate to butyrate and then caproate is not favourable. Similar results have also been observed in continuously syngas-fed bioreactors with *C. carboxidivorans* WT, using different growth temperatures and pH control strategies, confirming the absence of chain elongation pathway stimulation under not gas-limited condition, even in the

Table 1
Main metrics of reactor fermentation with different H_2 & CO_2 partial pressures (4:1). All data represent the average ± standard error of the mean (SEM) of duplicate experiments.

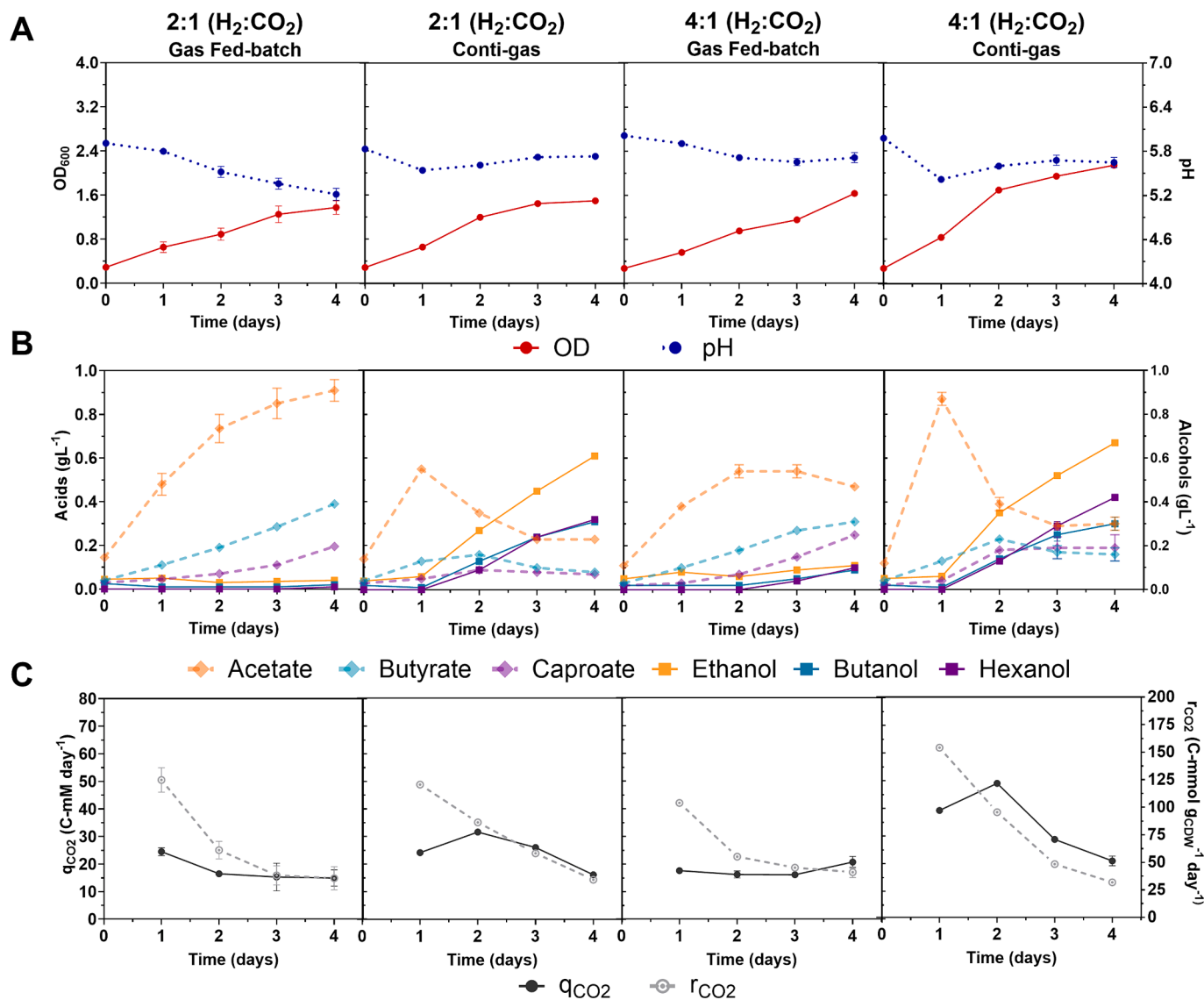|	Condition 1	Condition 2	Condition 3	Condition 4
	P tot = 1.5 p_{H2} = 0.6 p_{CO2} = 0.15 p_{N2} = 0.75	P tot = 1.5 p_{H2} = 1.2 p_{CO2} = 0.30	P tot = 1.8 p_{H2} = 1.44 p_{CO2} = 0.36	P tot = 3 p_{H2} = 2.40 p_{CO2} = 0.60
Biomass (gL^{-1}) at day 2	0.39 ± 0.04	0.38 ± 0.03	0.51 ± 0.00	0.53 ± 0.03
q_{CO2} at day 2 (C-mM day^{-1})	28.01 ± 1.96	30.73 ± 1.19	48.69 ± 0.68	55.58 ± 0.75
r_{CO2} at day 1 (C-mmol g_{CDW}^{-1} day^{-1})	152.24 ± 0.71	144.60 ± 1.23	154.16 ± 1.70	167.27 ± 2.01
Total alcohols (gL^{-1})	1.06 ± 0.13	1.73 ± 0.00	2.09 ± 0.11	2.55 ± 0.07
Alcohols: acids ratio	1.04	1.75	2.51	3.73
Acids consumed (gL^{-1})	0.20 ± 0.12	0.28 ± 0.00	0.53 ± 0.02	0.73 ± 0.07
Max r_{Acet} (g_{Acet} g_{CDW}^{-1}h^{-1})	0.129 ± 0.001	0.123 ± 0.003	0.129 ± 0.003	0.143 ± 0.001
Max −r_{Acet} (g_{Acet} g_{CDW}^{-1}h^{-1})	− 0.024 ± 0.000	− 0.022 ± 0.000	− 0.038 ± 0.000	− 0.046 ± 0.005
Max r_{EtOH} (g_{EtOH} g_{CDW}^{-1}h^{-1})	0.018 ± 0.002	0.021 ± 0.002	0.023 ± 0.001	0.039 ± 0.007
Max r_{HexOH} (g_{HexOH} g_{CDW}^{-1}h^{-1})	0.009 ± 0.001	0.008 ± 0.001	0.012 ± 0.001	0.010 ± 0.002

Fig. 2. Growth, product profiles and C-uptake rate with gas fed-batch and conti-gas with both 2:1 and 4:1 $H_2:CO_2$ gas ratio. (A) Optical density profiles (solid red lines), pH profiles (dotted blue lines) and (B) products profiles. Acetate, butyrate and caproate are respectively shown as light orange, light blue and light purple diamond shapes with dotted lines. Ethanol, butanol and hexanol are respectively shown as orange, blue and purple squares with solid lines. (C) Specific CO_2 uptake rate (r_{CO2}) (C-mmol g_{CDW}^{-1} day^{-1}) is shown as light gray dotted lines; volumetric CO_2 uptake rate (q_{CO2}) (C-mM day^{-1}) is shown as dark solid line. Data from 4:1 conti-gas, 4:1 gas fed-batch and 2:1 gas fed-batch represent the average ± standard error of the mean (SEM) of duplicate experiments. Data from 2:1 conti-gas represent a single experiment.

presence of CO (Rückel et al., 2021; Fernández-Naveira et al., 2017a).

During both 2:1 and 4:1 gas-fed batch fermentations, the CO_2 concentration measured in the reactor headspace progressively decreased, from 20 % and 33 % at the beginning of the test, respectively, to 1.6 % and 20 % at day 4. Similarly, the modeled abiotic CO_2 dissolution rate exhibited a decline, from 11.4 to 8.2 C-mM day^{-1} (2:1 fed-batch) and from 5.7 to 0.21 C-mM day^{-1} (4:1 fed batch) (see Supplementary Material). On the 4th day of the 2:1 gas fed-batch fermentation, the CO_2 uptake rate (Fig. 2) was two times higher than the abiotic CO_2 dissolution rate. This gap was even larger on the last day of the 4:1 gas fed-batch condition (about two orders of magnitude higher than the CO_2 uptake rate) (see supplementary material). Acids were the main products detected, with acetate being the predominant one. Particularly in the 2:1 condition, neither acid consumption nor alcohol production was observed, resulting in the highest total acid production (1.5 gL^{-1}) and a consequent pH decrease to 5.2 (Fig. 3).

Thus, when CO_2 is limiting in the liquid phase, the chain elongation metabolism of the strain is stimulated at the expense of solventogenesis.

This result is very interesting because the direct production of caproate from CO_2 and H_2 with acetogens had been reported only for very low concentrations (Thunuguntla et al., 2024a, Thunuguntla et al., 2024b). Furthermore, alcohols can be generated through the indirect pathway based on the acid conversion into the relative alcohol via the aldehyde oxidoreductase enzyme (AOR) (Fernández-Naveira et al., 2017a–c; Vees et al., 2022). Consequently, elevated concentrations of caproate in the fermentation broth can positively influence cell-specific hexanol productivity. This assumption was demonstrated in gas fed-batch serum bottles experiments with the external addition of caproate (see Supplementary Material). By adding 2 gL^{-1} of caproate, a maximum r_{HexOH} of 0.100 ± 0.005 g$_{HexOH}$ g$_{CDW}^{-1}$h^{-1} was observed, which is approximately 3.2-fold higher than the r_{HexOH} obtained in the absence of caproate addition (0.031 ± 0.005 g$_{HexOH}$ g$_{CDW}^{-1}$h^{-1}) (P value = 0.0033 (**)). The results obtained in this study can help to explain why the highest hexanol titers achieved in CO-fed serum bottles with gas-refill (Oh et al., 2022, 2023) have never been replicated in reactor environments, where gas has always been supplied continuously, keeping the microorganism
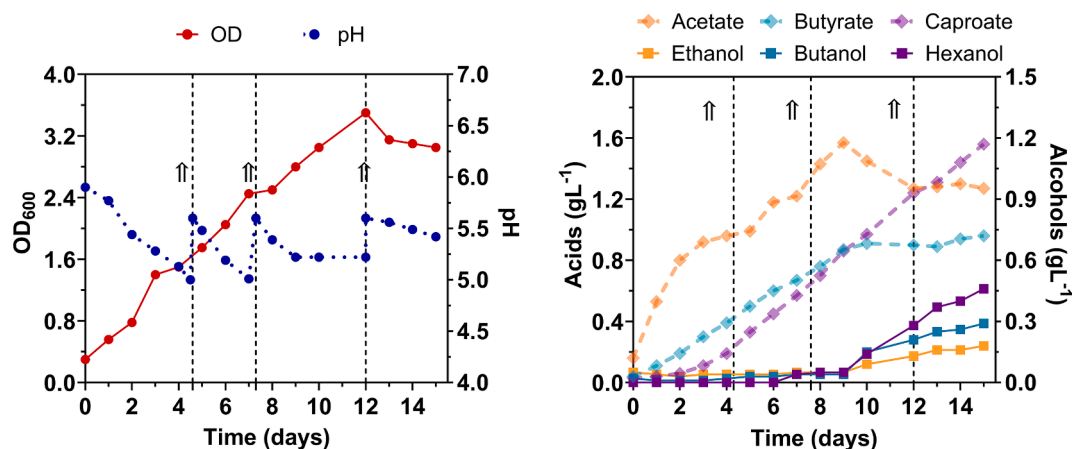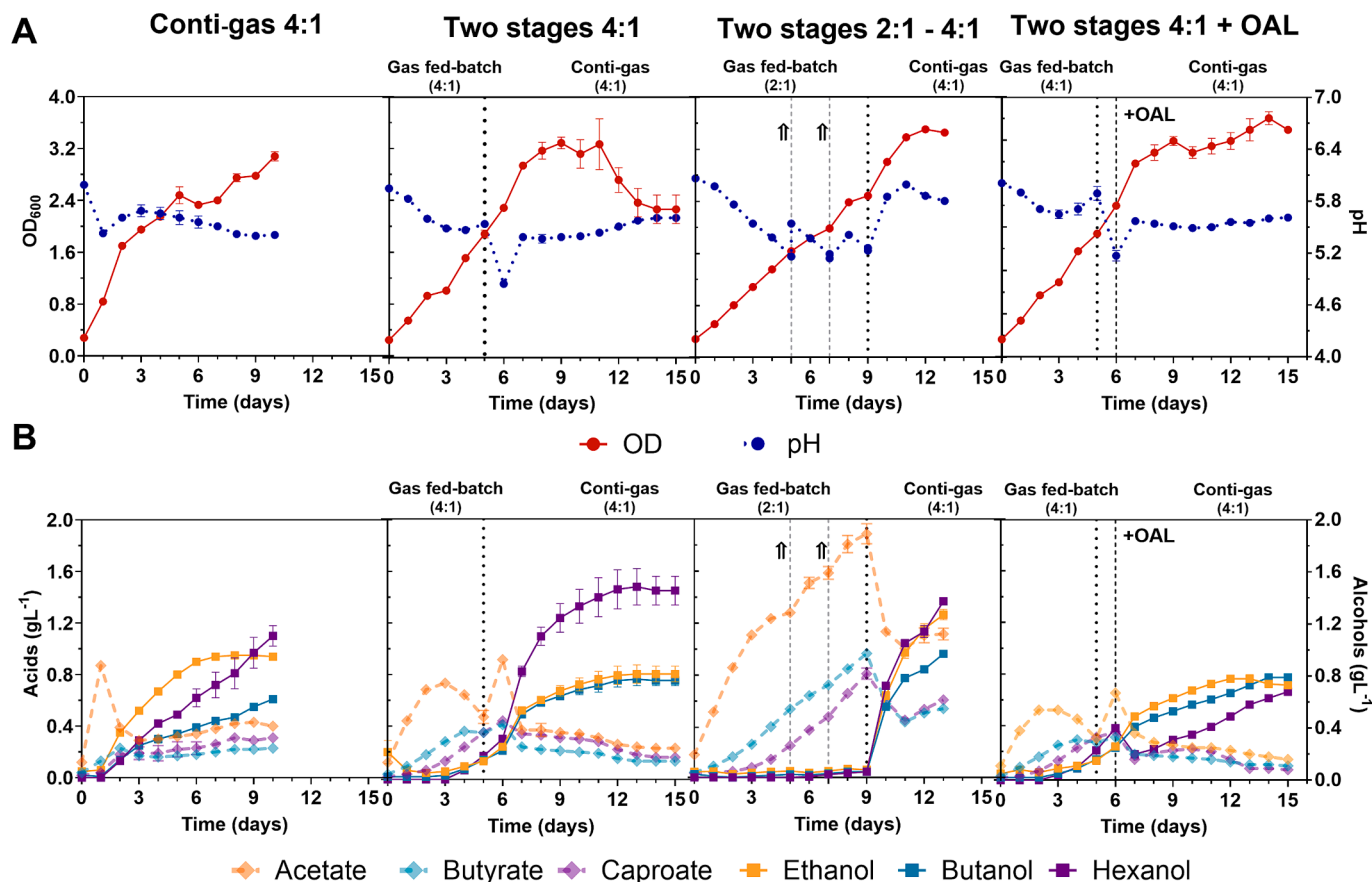
Fig. 3. Growth and product profiles with 2:1 (H₂:CO₂) in gas fed-batch with pH control. (A) Optical density profiles (solid red lines), pH profiles (dotted blue lines) and (B) products profiles. Acetate, butyrate and caproate are respectively shown as light orange, light blue and light purple diamond shapes with dotted lines. Ethanol, butanol and hexanol are respectively shown as orange, blue and purple squares with solid lines. All data derived from a single experiment.

consistently in a non-gas-limiting state (Doll et al., 2018; Lanzillo et al., 2024; Rückel et al., 2021; Shen et al., 2017; Vees et al., 2022).

To boost the chain elongation pathway of the adapted strain and to improve caproate production in the bioreactor, a longer fermentation experiment of 15 days was conducted, using the 2:1 gas fed-batch condition (Fig. 3). To prevent cell death due to acid crash, the pH in the reactors was increased to 5.6 each time it reached 5. The fermentation strategy was successful. Biomass increased to an OD₆₀₀ of 3.4 by day 12.

Alcohols production was limited, starting only after 9 days of fermentation, with hexanol being the predominant alcohol produced (0.5 gL⁻¹). Caproate emerged as the main product by the end of fermentation, achieving a carbon selectivity of 32 % and a final titer of 1.6 gL⁻¹, which represents the highest titer obtained *via* pure culture gas fermentation with acetogens. This phenotypic behavior raises many questions that can only be addressed through future metabolomic studies, alongside *in silico* modeling and flux balance analyses. Such

Fig. 4. Growth and product profiles in conti-gas (4:1), two stages (4:1), two stages (2:1 + 4:1) and two stages (4:1) with oleyl alcohol (OAL). (A) Optical density profiles (solid red lines), pH profiles (dotted blue lines) and (B) products profiles. Acetate, butyrate and caproate are respectively shown as light orange, light blue and light purple diamond shapes with dotted lines. Ethanol, butanol and hexanol are respectively shown as orange, blue and purple squares with solid lines. All data represent the average ± standard error of the mean (SEM) of duplicate experiments.

efforts will help elucidate the differences in intracellular metabolites and carbon and energy fluxes of the strain under gas-limited and non-gas-limited growth conditions, ultimately providing insights into the regulatory mechanisms governing the stimulation of the chain elongation pathway using CO_2 and H_2 as substrate.

3.3. Optimization of hexanol production through two-stage gas feeding strategy and in-situ solvent extraction

The outcomes achieved from the above screening campaign, allowed us to understand how to drive the strain to produce more caproate (gas fed-batch) at the expense of ethanol (conti-gas) in order to improve hexanol production performances. Therefore, to increase hexanol production in the reactor system, different two-stage gas feeding configurations were investigated, at a total pressure of 1.8 bar. Specifically, a strategy based on a gas fed-batch phase with an $H_2{:}CO_2$ ratio of 4:1 followed by a conti-gas phase with the same gas mixture (two stages 4:1) and a second strategy based on a gas fed-batch phase of 2:1 followed by a 4:1 conti-gas phase (two stages 2:1 + 4:1) have been investigated. In the latter configuration, during the gas fed-batch phase, the pH was increased to 5.6 each time it reached 5. Fig. 4 shows a comparison between the growth, pH and products profiles of the above-mentioned experiments and trends obtained in the single phase conti-gas fermentation condition (conti-gas 4:1). Both the two-stage configurations resulted in slower growth during the first days of fermentation, compared to the single gas feeding condition. During the first 3 days of the gas fed-batch phase with both the 4:1 and 2:1 H_2 to CO_2 ratio, the specific growth rate (μ) was respectively 1.5-fold and 1.4-fold lower compared to the conti-gas configuration (μ P < 0.0001(****) for both comparisons) (Table 2). Regarding the product profile, in the two-stage 4:1 fermentation, the conti-gas phase closely resembled the single phase conti-gas fermentation, showing acid consumption and a shift towards solventogenesis. In this case, however, since the conti-gas phase started with higher concentrations of caproate in the liquid (0.45 ± 0.00 gL^{-1}) (produced during the first fed-batch phase), the solventogenic phase was more selective towards hexanol due to its indirect production from caproate (Fig. 4B). Specifically, a hexanol carbon selectivity of 41 % was achieved, which is 1.3 times higher than in the single phase conti-gas fermentation (32 %) (P value = 0.0225 (*)) (Fig. 5). Furthermore, the maximum r$_{HexOH}$ achieved was doubled (0.024 ± 0.001 g$_{HexOH}$

g$_{CDW}^{-1}$h^{-1}) compared to the single phase conti-gas fermentation (0.012 ± 0.001 g$_{HexOH}$ g$_{CDW}^{-1}$h^{-1}) (P value = 0.0090 (**)). A maximum hexanol titer of 1.48 ± 0.14 gL^{-1} was reached by day 12 of fermentation.

In the two stages 2:1 + 4:1 fermentation condition, the conti-gas phase started after 9 days of 2:1 gas fed-batch phase, resulting in a caproate titer of 0.83 ± 0.06 gL^{-1}. During the gas fed-batch phase, very high concentrations of acetate and butyrate were also achieved, 1.89 ± 0.11 gL^{-1} and 0.96 ± 0.01 gL^{-1}, respectively. Consequently, the selectivity of the solventogenic pathway shifted towards the production of both ethanol and hexanol in the 4:1 conti-gas phase (Fig. 4B, Table 2). The ratio of alcohols, ethanol: butanol: hexanol, was 1:0.79:1.13. Thus, the hexanol carbon selectivity of this fermentation strategy (25 %) was 1.60 times lower than the one observed in the two stage 4:1 condition (41 %) (P value = 0.0014 (**)). However, the two-stage 2:1 + 4:1 condition provided the highest maximum cell-specific hexanol productivity achieved among all the tests in this study, reaching 0.038 ± 0.002 g$_{HexOH}$ g$_{CDW}^{-1}$h^{-1}. This value is 1.6 times higher than the r$_{HexOH}$ obtained in the two stage 4:1 fermentation strategy (P value = 0.0003 (***)) (Table 2) and 1.2 times higher than the highest r$_{HexOH}$ reported so far in literature in serum bottles (0.031 ± 0.005 g$_{HexOH}$ g$_{CDW}^{-1}$h^{-1}) (P value = 0.0172 (*)) (Antonicelli et al., 2023). Furthermore, the r$_{HexOH}$ obtained in this work is 1.4-fold higher compared to the value obtained in continuously syngas-fed bioreactors with pH control (0.026 g$_{HexOH}$ g$_{CDW}$ h^{-1}) (Fernández-Naveira et al., 2017a).

Among the two two-stage fermentation strategies, the 4:1 condition reached the highest hexanol carbon selectivity (41 %) and hexanol titer (1.48 ± 0.14 gL^{-1}) on day 12. After day 12, the microbial culture started to die (Fig. 4A), most likely due to the toxic effects of hexanol on cells. Kottenhahn and colleagues previously assessed the toxic effect of hexanol on cell growth. At 30 °C, they calculated the half-maximal inhibitory concentration (IC$_{50}$) to be 1.7 gL^{-1} (Kottenhahn et al., 2021). To increase the production of hexanol and overcome inhibition, a two-stage 4:1 fermentation experiment with the use of OAL, as a selective solvent for in-situ hexanol extraction, was performed. In the literature, the OAL addition in CO-fed serum bottles provided a very high hexanol titer, reaching the remarkably high concentration of 5 gL^{-1} (Oh et al., 2023). In order to improve the hexanol production by C.carboxidivorans_hex21 from CO_2 and H_2, 6 % v/v of OAL was added after the first day of the conti-gas phase (day 6) (Fig. 4). The hexanol titer in the medium phase slightly increased until the end of the fermentation, reaching 0.68 ± 0.01 gL^{-1}. The growth profile demonstrates that keeping the hexanol concentration below toxic levels could prevent biomass death after day 12, as compared to the test without OAL (Fig. 4A). At the end of the fermentation, the hexanol titer in the OAL phase was measured. C. carboxidivorans_hex21 was able to produce a total of 3.65 ± 0.04 gL^{-1} of hexanol (liquid medium = 0.68 ± 0.01 gL^{-1}; OAL phase = 2.96 ± 0.04 gL^{-1}) (Fig. 5A). This titer is about 2.5 times higher compared to the two-stages 4:1 condition without OAL (P value < 0.0001 (****)) (Table 2) (Fig. 5A). This is the highest hexanol titer obtained so far in bioreactor with acetogenic bacteria. Furthermore, the alcohols to acids ratio was 15.43 ± 0.81, which is about 2.8 times higher than the ratio obtained without OAL (P value = 0.0079 (**)) (Table 2). The solvent selectivity for hexanol extraction among other alcohols was also confirmed, although a small concentration of butanol (0.24 gL^{-1}) and traces of octanol were found in the OAL phase (data not shown). The hexanol carbon selectivity at the end of this fermentation was 60 %, which is the highest value reported to date in gas fermentation (Fig. 5B).

Gas fermentation processes, to be scaled and economically viable, must achieve a product selectivity of 90 % and maintain stable volumetric productivity values in the range of g L^{-1}h^{-1} (Köpke & Simpson, 2020). Although this study has not reached these values yet, the results presented here are extremely promising, with significant potential for further optimization of the process. For instance, based on the max r$_{HexOH}$ achieved (0.04 g$_{HexOH}$ g$_{CDW}^{-1}$h^{-1}), the hexanol volumetric productivity could be enhanced to the range of gL^{-1}h^{-1} by adopting a continuous cell recycling system to retain and concentrate biomass

Table 2
Main metrics of reactor fermentations in single phase conti-gas, two stages 4:1, two stage 2:1 + 4:1 and two stages with oleyl alcohol. All data represent the average ± standard error of the mean (SEM) of duplicate experiments.
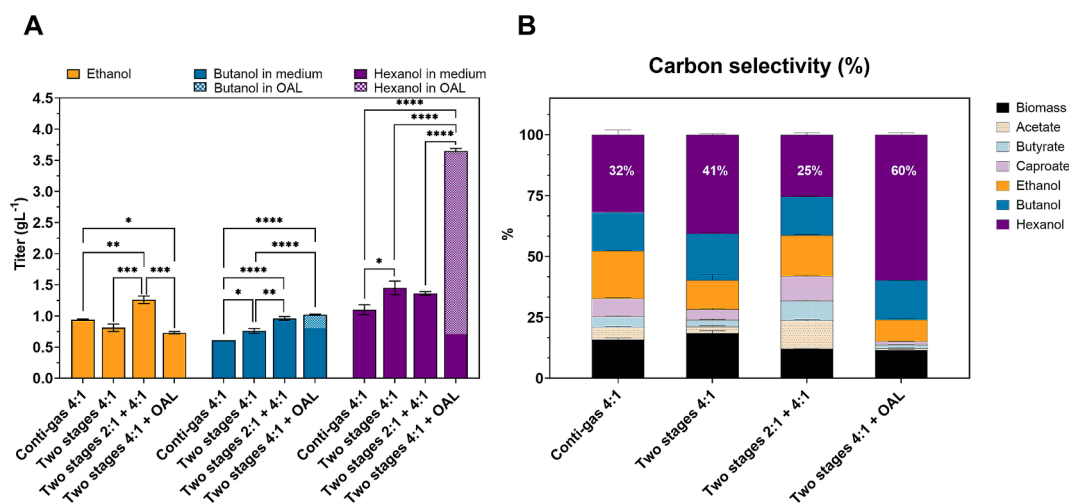
	Conti-gas 4:1	Two stages 4:1	Two stages 2:1 + 4:1	Two stages + OAL
μ first 3 days (h^{-1})	0.027 ± 0.001 R^2: 0.97	0.019 ± 0.000 R^2: 0.96	0.020 ± 0.001 R^2: 0.99	0.020 ± 0.001 R^2: 0.99
Max Biomass (gL^{-1})	0.92 ± 0.02	0.99 ± 0.03	1.05 ± 0.01	1.10 ± 0.03
Total alcohols (gL^{-1})	2.65 ± 0.10	3.02 ± 0.22	3.52 ± 0.06	5.40 ± 0.01
Alcohols: acids ratio	2.82 ± 0.20	5.42 ± 0.43	1.60 ± 0.02	15.16 ± 0.81
Max q$_{HexOH}$ (gL^{-1}h^{-1})	0.007 ± 0.001	0.022 ± 0.001	0.034 ± 0.001	n.a.
Max r$_{HexOH}$ (g$_{HexOH}$ g$_{CDW}^{-1}$h^{-1})	0.012 ± 0.001	0.024 ± 0.001	0.038 ± 0.002	n.a.
Max q$_{Capr}$ (gL^{-1}h^{-1})	0.006 ± 0.001	0.005 ± 0.001	0.012 ± 0.002	0.004 ± 0.000
Max r$_{Capr}$ (g$_{Capr}$ g$_{CDW}^{-1}$h^{-1})	0.011 ± 0.001	0.011 ± 0.001	0.020 ± 0.004	0.008 ± 0.000
etOH:butOH: hexOH	1:0.65:1.17	1:0.94:1.78	1:0.79:1.13	1:1.41:5.03

Fig. 5. (A) Statistical analysis of maximum alcohols titers obtained in conti-gas (4:1), two stages (4:1), two stages (2:1 + 4:1) and two stages (4:1) with oleyl alcohol (OAL). The amount of alcohols in solvent phase are shown with square pattern. All data represent the average ± standard error of the mean (SEM) of duplicate experiments. The ordinary one-way ANOVA is performed for figure A. (p < 0.0332(*) p < 0.0021 (**) p < 0.0002 (***) p < 0.0001 (****)). (B) Final carbon selectivity in the conditions tested. All data represent the average of duplicate experiments.

within the reactor. Additionally, the r_{HexOH} can be increased by further improving the caproate production phase of the strain, as demonstrated in serum bottles experiment with external addition of this acid. Furthermore, it is crucial to develop a continuous product downstream process that is energetically favorable, selective for hexanol with respect to by-products, and easily scalable to handle commercial-scale reactor fermentation broths (e.g. 500 m^3). In terms of product selectivity, valorizing the mixture of by-products (acetate, butyrate, caproate, ethanol, and butanol) as a substrate for a secondary bioprocess selective for the production of other value-added compounds could significantly enhance the economic feasibility of bio-hexanol production via gas fermentation technology.

4. Conclusion

This study demonstrated the close interconnection between different CO_2 and H_2 feeding conditions and the stimulation of distinct product pathways in an adapted *C. carboxidivorans* strain cultivated in elevated-pressure reactors. The two-stage gas feeding strategy proved to be an effective approach for achieving the highest hexanol cell-specific productivity (0.9 $g g_{CDW}^{-1}$ day^{-1}) and selectivity (60 %) reported to date in the literature. These findings broaden the range of products generated in lab-scale bioreactors using CO_2 and H_2. In particular, it paves the way for scaling-up gas fermentation processes that can generate products beyond ethanol and acetate while valorizing feedstocks without CO.

CRediT authorship contribution statement

G. Antonicelli: Writing – review & editing, Writing – original draft, Visualization, Methodology, Investigation, Formal analysis, Conceptualization. **N. Vasile:** Writing – review & editing, Supervision, Methodology, Investigation, Formal analysis. **E. Piro:** Writing – review & editing, Investigation. **S. Fraterrigo Garofalo:** Writing – review & editing, Methodology, Investigation. **B. Menin:** Writing – review & editing, Resources. **F. Verga:** Writing – review & editing, Supervision. **F. Pirri:** Writing – review & editing, Funding acquisition. **V. Agostino:** Writing – review & editing, Writing – original draft, Visualization, Validation, Supervision, Resources, Project administration, Methodology, Investigation, Conceptualization.

Declaration of competing interest

The authors declare that they have no known competing financial interests or personal relationships that could have appeared to influence the work reported in this paper.

Appendix A. Supplementary data

Supplementary data to this article can be found online at https://doi.org/10.1016/j.biortech.2024.131966.

Data availability

Data will be made available on request.

References

Abubackar, H. N., Veiga, M. C., Kennes, C., 2018. Production of Acids and Alcohols from Syngas in a Two-Stage Continuous Fermentation Process. Bioresource Technology (253(November 2017):), 227–34. doi:10.1016/j.biortech.2018.01.026.

Akita, Kiyomi, and Fumitake Yoshidal. n.d. *Gas Holdup and Volumetric Mass Transfer Coefficient in Bubble Columns Effects of Liquid Properties.*

Antonicelli, G., Ricci, L., Tarraran, L., Fraterrigo Garofalo, S., Re, A., Vasile, N.S., Verga, F., Pirri, C.F., Menin, B., Agostino, V., 2023. Expanding the product portfolio of carbon dioxide and hydrogen-based gas fermentation with an evolved strain of *Clostridium Carboxidivorans*. Bioresour. Technol. 387. https://doi.org/10.1016/j.biortech.2023.129689.

Bae, Jiyun, Yoseb Song, Hyeonsik Lee, Jongoh Shin, Sangrak Jin, Seulgi Kang, and Byung Kwan Cho. 2022. 'Valorization of C1 Gases to Value-Added Chemicals Using Acetogenic Biocatalysts'. *Chemical Engineering Journal* 428.

Doll, K., Rückel, A., Kämpf, P., Wende, M., Weuster-Botz, D., 2018. Two stirred-tank bioreactors in series enable continuous production of alcohols from carbon monoxide with *Clostridium carboxidivorans*. Bioprocess Biosyst. Eng. 41 (10), 1403–1416. https://doi.org/10.1007/s00449-018-1969-1.

Fernández-Blanco, C., Robles-Iglesias, R., Naveira-Pazos, C., Veiga, M.C., Kennes, C., 2023. Production of biofuels from C1-gases with *Clostridium* and related bacteria—recent advances. J. Microbial. Biotechnol. 16 (4), 726–741. https://doi.org/10.1111/1751-7915.14220.

Fernández-Naveira, Á., Abubackar, H.N., Veiga, M.C., Kennes, C., 2017a. Production of chemicals from C1 Gases (CO, CO₂) by *Clostridium Carboxidivorans*. World J. Microbiol. Biotechnol. 33 (3). https://doi.org/10.1007/s11274-016-2188-z.

Fernández-Naveira, Á., Veiga, M.C., Kennes, C., 2017b. Effect of PH control on the anaerobic H-B-E fermentation of syngas in bioreactors. J. Chem. Technol. Biotechnol. 92 (6), 1178–1185. https://doi.org/10.1002/jctb.5232.

Fernández-Naveira, Á., Veiga, M.C., Kennes, C., 2017c. H-B-E (Hexanol-Butanol-Ethanol) fermentation for the production of higher alcohols from syngas/waste gas. J. Chem. Technol. Biotechnol. 92 (4), 712–731. https://doi.org/10.1002/jctb.5194.

Garcia-Ochoa, F., Gomez, E., 2009. Bioreactor scale-up and oxygen transfer rate in microbial processes: an overview. *Biotechnol. Adv.* 27 (2), 153–176.

Heffernan, J.K., Valgepea, K., de Souza, R., Lemgruber, P., Casini, I., Plan, M., Tappel, R., Simpson, S.D., Köpke, M., Nielsen, L.K., Marcellin, E., 2020. Enhancing CO2-valorization using *Clostridium Autoethanogenum* for sustainable fuel and chemicals production. *Front. Bioeng. Biotechnol.* 8 (March), 1–10. https://doi.org/10.3389/fbioe.2020.00204.

Hermann, M., Teleki, A., Weitz, S., Niess, A., Freund, A., Bengelsdorf, F.R., Takors, R., 2020. Electron availability in CO2, CO and H2 mixtures constrains flux distribution, energy management and product formation in *Clostridium Ljungdahlii. J. Microbial. Biotechnol.* 13 (6), 1831–1846. https://doi.org/10.1111/1751-7915.13625.

Huang, T., Ma, Y., 2023. Advances in biosynthesis of higher alcohols in *Escherichia Coli. World J. Microbiol. Biotechnol.* 39 (5).

IPCC. 2023. 'Section 4: Near-Term Responses in a Changing Climate'. *Climate Change 2023: Synthesis Report* 42–66. doi: 10.59327/IPCC/AR6-9789291691647.

Kim, Ji Yeon, Mungyu Lee, Soyoung Oh, Byeongchan Kang, Muhammad Yasin, and In Seop Chang. 2023. 'Acetogen and Acetogenesis for Biological Syngas Valorization'. *Bioresource Technology* 384.

Köpke, M., Simpson, S.D., 2020. Pollution to products: recycling of "above ground" carbon by gas fermentation. *Curr. Opin. Biotechnol.* 65, 180–189. https://doi.org/10.1016/j.copbio.2020.02.017.

Kottenhahn, P., Philipps, G., Jennewein, S., 2021. Hexanol biosynthesis from syngas by *Clostridium Carboxidivorans* P7 – Product toxicity, temperature dependence and in situ extraction. *Heliyon* 7 (8), e07732. https://doi.org/10.1016/j.heliyon.2021.e07732.

Lanzillo, F., S. Pisacane, M. Capilla, F. Raganati, M. E. Russo, P. Salatino, and A. Marzocchella. 2024. 'Continuous H-B-E Fermentation by *Clostridium Carboxidivorans*: CO vs Syngas'. *New Biotechnology* 81(October 2023):1–9. doi: 10.1016/j.nbt.2024.02.004.

Liou, J.S.C., Balkwill, D.L., Drake, G.R., Tanner, R.S., 2005. *Clostridium Carboxidivorans* Sp. nov., a solvent-producing *Clostridium* Isolated from an agricultural Settling Lagoon, and Reclassification of the Acetogen *Clostridium Scatologenes* strain SL1 as *Clostridium Drakei* Sp. Nov. *Int. J. Syst. Evol. Microbiol.* 55 (5), 2085–2091. https://doi.org/10.1099/ijs.0.63482-0.

Mock, J., Zheng, Y., Mueller, A.P., Ly, S., Tran, L., Segovia, S., Nagaraju, S., Köpke, M., Dürre, P., Thauer, R.K., 2015. Energy Conservation Associated with Ethanol Formation from H2 and CO2 in *Clostridium Autoethanogenum* Involving Electron Bifurcation. *J. Bacteriol.* 197 (18), 2965–2980. https://doi.org/10.1128/JB.00399-15.

Oh, H.J., Ko, J.K., Gong, G., Lee, S.M., Um, Y., 2022. Production of hexanol as the main product through syngas fermentation by *Clostridium Carboxidivorans* P7. *Front. Bioeng. Biotechnol.* 10. https://doi.org/10.3389/fbioe.2022.850370.

Oh, H.J., Gong, G., Ahn, J.H., Ko, J.K., Lee, S.M., Um, Y., 2023. Effective hexanol production from carbon monoxide using extractive fermentation with *Clostridium Carboxidivorans* P7. *Bioresour. Technol.* 367. https://doi.org/10.1016/j.biortech.2022.128201.

Di Leonardo PF, Antonicelli G, Agostino V, Re A. Genome-Scale Mining of Acetogens of the Genus *Clostridium* Unveils Distinctive Traits in [FeFe]- and [NiFe]-Hydrogenase Content and Maturation. Microbiol Spectr. 2022 Aug 31;10(4):e0101922. doi: 10.1128/spectrum.01019-22.

Phillips, J.R., Atiyeh, H.K., Tanner, R.S., Torres, J.R., Saxena, J., Wilkins, M.R., Huhnke, R.L., 2015. Butanol and hexanol production in *Clostridium Carboxidivorans* syngas fermentation: medium development and culture techniques. *Bioresour. Technol.* 190, 114–121. https://doi.org/10.1016/j.biortech.2015.04.043.

Ramió-Pujol, S., Ganigué, R., Bañeras, L., Colprim, J., 2015. Incubation at 25°C prevents acid crash and enhances alcohol production in *Clostridium Carboxidivorans* P7. *Bioresour. Technol.* 192, 296–303. https://doi.org/10.1016/j.biortech.2015.05.077.

Riegler, P., Chrusciel, T., Mayer, A., Doll, K., Weuster-Botz, D., 2019. Reversible retrofitting of a stirred-tank bioreactor for gas-lift operation to perform synthesis gas fermentation studies. *Biochem. Eng. J.* 141, 89–101. https://doi.org/10.1016/j.bej.2018.09.021.

Oswald F. Katharina Stoll M. Zwick S. Herbig J. Sauer N. Boukis A. Neumann Formic Acid Formation by Clostridium Ljungdahlii at Elevated Pressures of Carbon Dioxide and Hydrogen Frontiers in Bioengineering and Biotechnology 6(FEB) 2018 10.3389/fbioe.2018.00006.

Rückel, A., Oppelt, A., Leuter, P., Johne, P., Fendt, S., Weuster-Botz, D., 2022. Conversion of Syngas from Entrained Flow Gasification of Biogenic Residues with *Clostridium Carboxidivorans* and *Clostridium Autoethanogenum*. Fermentation 8 (9). https://doi.org/10.3390/fermentation8090465.

Rückel, A., Hannemann, J., Maierhofer, C., Fuchs, A., Weuster-Botz, D., 2021. Studies on syngas fermentation With *Clostridium Carboxidivorans* in stirred-tank reactors with defined gas impurities. *Front. Microbiol.* 12, 1–16. https://doi.org/10.3389/fmicb.2021.655390.

Sander, R., 2023. Compilation of Henry's Law Constants (Version 5.0.0) for Water as Solvent. *Atmos. Chem. Phys.* 23 (19), 10901.

Schuchmann K., Chowdhury N. P., and Müller V. 2018. 'Complex Multimeric [FeFe] Hydrogenases: Biochemistry, Physiology and New Opportunities for the Hydrogen Economy'. *Frontiers in Microbiology* 9(DEC):1–22. doi: 10.3389/fmicb.2018.02911.

Shen, Y., Brown, R., Wen, Z., 2014a. Enhancing mass transfer and ethanol production in syngas fermentation of *Clostridium Carboxidivorans* P7 through a monolithic biofilm reactor. *Appl. Energy* 136, 68–76. https://doi.org/10.1016/j.apenergy.2014.08.117.

Shen, Y., Brown, R., Wen, Z., 2014b. Syngas fermentation of *Clostridium Carboxidivoran* P7 in a hollow fiber membrane biofilm reactor: evaluating the mass transfer coefficient and ethanol production performance. *Biochem. Eng. J.* 85, 21–29. https://doi.org/10.1016/j.bej.2014.01.010.

Shen, Y., Brown, R.C., Wen, Z., 2017. Syngas fermentation by *Clostridium Carboxidivorans* P7 in a horizontal rotating packed bed biofilm reactor with enhanced ethanol production. *Appl. Energy* 187, 585–594. https://doi.org/10.1016/j.apenergy.2016.11.084.

Sun, X., Atiyeh, H.K., Huhnke, R.L., Tanner, R.S., 2019. Syngas fermentation process development for production of biofuels and chemicals: a review. *Bioresour. Technol. Rep.* 7.

Tarraran L., Agostino V., Vasile N. S., Abdel Azim A., Antonicelli G., Baker J., Millard J., Re A., Menin B., Tommasi T., Minton N. P., Pirri C. F. , and Fino D. 2023. 'High-Pressure Fermentation of CO2 and H2 by a Modified *Acetobacterium Woodii*'. *Journal of CO2 Utilization* 76(September). doi: 10.1016/j.jcou.2023.102583.

Tarraran, L., Lueckel, F.B., Tommasi, T., Contador, F.I.S., Fino, D., 2022. A practical method for gas changing time estimation using a simple gas-liquid mass transfer model. *J. Microbiol. Methods* 200, 106544. https://doi.org/10.1016/J.MIMET.2022.106544.

Thunuguntla, R., Atiyeh, H.K., Huhnke, R.L., Tanner, R.S., 2024a. CO2-based production of C2-C6 acids and alcohols: the potential of novel *Clostridia. Bioresour. Technol. Rep.* 25, 101713. https://doi.org/10.1016/j.biteb.2023.101713.

Thunuguntla, R., Atiyeh, H.K., Zhang, H., Ezeji, T.C., Tanner, R.S., 2024b. Biochar Facilitated Biological CO2 Conversion to C2-C6 Alcohols and Fatty Acids. *Bioresour. Technol.* 397, 130464. https://doi.org/10.1016/j.biortech.2024.130464.

Vees, C.A., Herwig, C., Pflügl, S., 2022. Mixotrophic co-utilization of glucose and carbon monoxide boosts ethanol and butanol productivity of continuous *Clostridium Carboxidivorans* Cultures. *Bioresour. Technol.* 353 (March), 127138. https://doi.org/10.1016/j.biortech.2022.127138.

Van't Riet, K. 1979. Review of Measuring Methods and Results in Mass Transfer in Stirred Vessels Nonviscous Gas-Liquid. Vol. 18.*Ind. Eng. Chem. Process Des. Dev.* 1979, 18, 3, 357–364.

Wirth, S., and Dürre P. 2021. 'Investigation of Putative Genes for the Production of Medium-Chained Acids and Alcohols in Autotrophic Acetogenic Bacteria'. *Metabolic Engineering* 66(December 2020):296–307. doi: 10.1016/j.ymben.2021.04.010.

Villadsen, J., Nielsen, J., Lidén, G.., 2011. *Bioreaction Engineering Principles*, Third Edition.

Wu, K.-K., Pian-Pian, Xu., Zhao, L., Ren, N.-Q., Zhang, Y.-F., 2024. Microbial conversion of carbon dioxide into premium medium-chain fatty acids: the progress, challenges, and prospects. *Npj Mater. Sustain.* 2 (1), 1–10. https://doi.org/10.1038/s44296-024-00008-w.

Xu, Y., Nie, G., Jiang, X., Wang, H., Yang, G., Yan, Z., Zou, J.J., Hailong, Yu., Shitao, Yu., Liu, Yu., 2024. Synthesis of 1-hexanol by highly selective hydrodeoxygenation of 5-hydroxymethylfurfural using Ni/MCM-41 and Pt-WOX/t-ZrO2. *Chem. Eng. J.* 487, 150695. https://doi.org/10.1016/j.cej.2024.150695.

Zedníková M., Orvalho S., Fialová M., and Ruzicka M. C.. n.d. 'Measurement of Volumetric Mass Transfer Coefficient in Bubble Columns'. doi: 10.3390/2020019.